

## **PORE-SCALE FINGERING DURING VISCIOUS OIL DISPLACEMENT**

Shashvat Doorwar, Kishore K. Mohanty, The University of Texas at Austin

*This paper was prepared for presentation at the International Symposium of the Society of Core Analysts held in Austin, Texas, USA 18-21 September, 2011*

### **ABSTRACT**

Recent research suggests that injecting chemicals (a combination of surfactant and alkali) after a short waterflood can improve recovery of very viscous oils (of the order of 10,000 cp) without excessive pressure drop. This research is aimed at the mechanistic understanding of these processes at the pore-scale. Several water floods, polymer flood and alkaline-surfactant floods have been conducted in a silicon micromodel. Visualization of the pore-scale displacement shows that viscosity ratio controls the finger structure. As the viscosity ratio increases, the number of growing fingers (or branches) before breakthrough decreases. At viscosity ratios of  $10^3$  or greater, the finger structure resembles DLA type fractal structures. Injection of alkaline-surfactant solution after waterflood lowers the interfacial tension and forms oil-in-water emulsion at the sides of previously established water fingers. The tertiary oil recovery due to alkaline-surfactant flood increases with the surface area of the water fingers.

### **INTRODUCTION**

The increased global energy demand and the difficulty in finding new conventional light oil reservoirs have shifted the focus of the upstream petroleum engineering research towards heavy and extra heavy oil reserves. It is estimated that out of the total world oil reserves of 9-13 trillion barrels of oil in place only 30% is conventional oil, 40% is heavy and extra heavy oil, and the remaining 30% is oil shale and bitumen [1]. The thermal methods such as SAGD and cyclic steam stimulation [2] are traditionally applied for production of such heavy oil. However, these thermal methods become infeasible and uneconomical when the reservoir is close to the permafrost, relatively thin or off-shore with no steam generation facility. Thus it is imperative to develop a nonthermal EOR process for improved recovery for viscous oils.

Cold heavy oil production with sand (CHOPS) is a nonthermal technique to produce viscous oil, but the ultimate recovery is between 5-8% [3]. Solvent processes can be applied to viscous oils, e.g., Vapex, but need high vertical permeability, availability of solvents and they are expensive [4]. Waterflooding can be applied but the high viscosity ratio leads to viscous fingering, early breakthrough, and low sweep [5]. There is a large

amount of published literature on immiscible displacement of viscous oils by water. Patterson [6] was the first to discuss the analogies of the (miscible) finger patterns with the fractal structures created by diffusion limited aggregation (DLA) models. In the DLA model, one starts with an occupied site (or seed) of a lattice located at the injection point. Random walkers are released, one at a time far from the seed site and are allowed to move randomly in the lattice. If a walker comes to an empty site adjacent to an occupied site, then the empty site is occupied and the aggregate of the occupied sites advances by one site. This walker is then removed and a new walker is released. The fractal dimension of a DLA cluster is 1.7 in 2D and 2.45 in 3D. DLA is applicable specifically for the case of infinite viscosity ratio.

Chen and Wilkinson [7], Lenormand et al. [8], and Lenormand [9] have discussed fingering patterns in great details for different viscosity ratios and capillary numbers. At a low capillary number, the displacement is controlled by capillarity and the pore scale displacement pattern is described by invasion-percolation (IP) algorithms. In the invasion-percolation model, the lattice is first filled with the displaced fluid called the *defender*. Each site of the lattice is assigned a random number uniformly distributed between 0 and 1 (which can be related to the resistance the defender offers to the invading fluid at the site). Then the displacing fluid, or the *invader*, is injected at the injection port. At each time step, it displaces the defender from one site at the interface that has the smallest random number. This process simulates drainage process in porous media at low viscosity ratio and low capillary number. The fractal dimension of the invasion percolation cluster is 1.82 in 2D and 2.5 in 3D.

The goal of this work is to develop chemical methods for viscous oil recovery which can improve upon waterfloods. Chemical methods include injection of polymers, surfactant, and alkali to improve the oil recovery. Polymers increase the viscosity of injected water and improve the sweep efficiency [10]. If the oil viscosity is below 1000 cP, it is possible to get high sweep and high enough injectivity. Polymer flooding should be applied as early as possible, e.g. as a secondary flooding technique. Surfactants reduce interfacial tension, mobilize oil and reduce residual oil saturation. This technique has been applied to many light oil reservoirs [11] and being considered for oil reservoirs of several 100 cP viscosity. The alkali can mix with acidic crudes to form in situ soap that can reduce interfacial tension, reduce surfactant adsorption, and increase the salinity [12]. Alkali-surfactant-polymer processes can achieve high sweep efficiency as well as high displacement efficiency in light oil reservoirs.

Recently, Bryan & Kantzas [13] and Kumar & Mohanty [14] have extended chemical flooding techniques to heavy oils (about 10,000 cP). They show that water breaks

through early (less than 10% PV) in sand pack waterfloods, but a significant amount of oil is recovered after the breakthrough. Waterflood recovery is about 20-30% PV in about 3 PV injection and it increases as the flow rate decreases. Injection of alkali-surfactant solution after 3 PV of water injection recovers another 20-40% PV of oil. As the salinity of the brine increases, oil recovery due to surfactant coreflood increases. Both oil-in-water and water-in-oil emulsions were produced in these core floods. A hydrophilic surfactant was used in these experiments, as these surfactants are expected to produce oil-in-water emulsions [15]. The mechanisms of alkaline-surfactant flood and even high viscosity ratio waterfloods are not clear from these core-scale experiments. The objective of this work is to better understand these mechanisms by conducting these floods in a visual micromodel.

In this paper, we conduct micromodel studies to understand high viscosity ratio waterfloods and subsequent alkaline-surfactant (AS) floods. The micromodel setup and fluids used are described in the next section. The results from these studies are discussed in the following section. The last section summarizes our conclusions.

## **METHODOLOGY**

The experiments were conducted in a two-dimensional porous medium (micro-model) etched on a silica plate. Such micromodels have been extensively used in pores scale petroleum engineering research as a surrogate porous medium [16-17]. The etched pattern on the micromodels covered 5cm X 5cm area and the pores were approximately 25  $\mu\text{m}$  deep. The average pore throat size was estimated to be about 50  $\mu\text{m}$ . The etched surface of the model was covered by a piece of glass. This enables us to visualize the oil and water movements using a reflection microscope. Figure 1(a) below shows a picture of the pores of the micromodel and Figure 1(b) shows the micromodel inside the flow cell. To prepare the micromodel for the water flooding experiment, we followed the procedure conventionally followed for a core flooding experiment as closely as possible, keeping in mind the pressure and force limits of our system. The micromodel was first vacuumed by pumping the air out with a syringe. Once the piston of the syringe can no longer be drawn further, the valve on the other end of the flow cell was opened. The synthetic reservoir brine rushed in and saturated the system. Oil was then injected to the system to displace the brine leaving behind some connate water. This oil saturated system was used for final water flooding experiments. The fluids were injected at the top left corner and produced from the bottom right corner. There was a wide flow channel on the top to distribute the fluids across the width (and a similar channel at the bottom). The experimental setup has been shown in the Figure 2. A microinjection pump was used to pump the liquid in the model at a constant rate of 5 $\mu\text{l}/\text{min}$ . This rate corresponds to be approximately 2.5 ft/d for our micromodel.

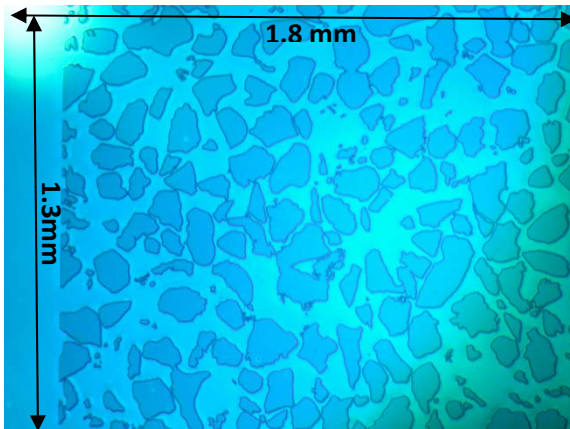


Figure 1(a). Microscopic view of the 1.8 mm X 1.3 mm section of the micromodel showing the etched pore pattern.

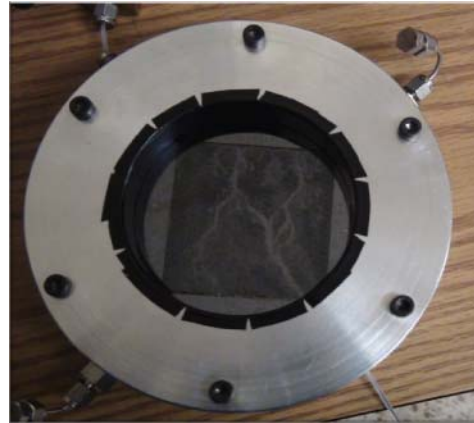


Figure 1(b). Micromodel inside the flow cell

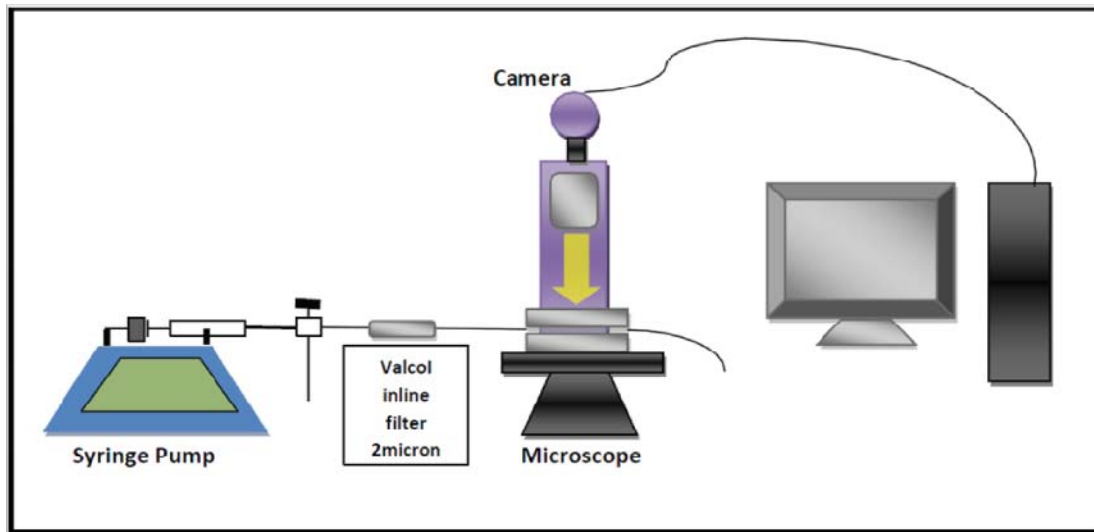


Figure 2. Experimental setup, micromodel, flowcell integrated with the image acquisition system.

Table 1: List of materials

Materials	Properties
Heavy oils	Viscosity of 10000 and 1000 cP
Light oil	Viscosity of 6 cP
NaCl brine for flooding	20000 ppm NaCl
3000 ppm of 3630S HPAM in water	Viscosity of 100 cP
Alkaline-surfactant slug	0.1% TDA-nEO, 2% NaCl, and 1.5% Na <sub>2</sub> CO <sub>3</sub>
50% glycerol and 50% water	Viscosity of 6 cP

Table 2: List of experiments

No.	Description of the Experiment	Recovery Mode
1	10,000 cp oil displaced with brine	Secondary
2	AS flood of 10000 cp oil after Exp. 1	Tertiary
3	10,000 cp oil displaced with 100 cp HPAM polymer	Secondary
4	AS flood of 10000 cp oil after Exp. 1	Tertiary
5	1000 cp oil with water	Secondary
6	6 cp oil displaced with 6 cp glycerol water	Secondary

Table 1 presents the list of materials used for our experiments. Six experiments were conducted and they are listed in Table 2. The experiments were recorded using a normal video camera. However, when higher resolution and pore level details were required, the setup was shifted under the microscope. The microscope had the capability to capture still images at high resolution. All the results and conclusions presented in this paper are derived from observations made during the course of the experiment. The analysis has been qualitative so far.

## RESULTS

This section has been divided into two different categories of experiments, namely secondary flooding and tertiary flooding. In the secondary flooding section, we discuss the case of water or polymer injection into the porous media saturated with oils of different viscosity. In the tertiary flooding section, we describe the effect of injection of alkali surfactant solution on the already water flooded medium.

### Secondary Floods

6 cP Oil Displaced by 6 cP Glycerol Water Solution ( $\mu_r = 1$ )

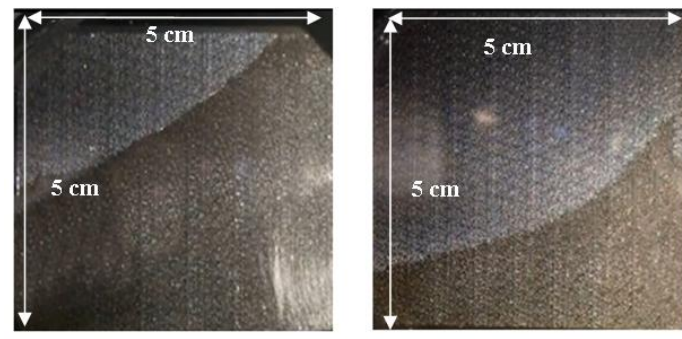


Figure 3. Water saturation front for unit viscosity ratio displacement after the injection of 7 $\mu$ l and 25  $\mu$ l. Water injected at top left corner and producer at the bottom right corner.

This experiment was conducted just to illustrate stable flow through the micromodel. In this experiment, the micro-model was first saturated with a light reservoir oil of viscosity about 6 cP. The oil was then displaced by a glycerol water solution of about the same viscosity. The viscosity ratio ( $\mu_r$ ) between the displaced and the displacing fluids was one. The water distribution is shown in Figure 3 at two different times. As expected the displacement front is very stable and moves through the micromodel from the left top corner to the bottom right corner. Viscous fingering or any kind of instability due to the non-homogeneity in the micro-model was not observed.

#### 10000 cP Oil Displaced with 1 cP Water ( $\mu_r = 10,000$ )

2% NaCl brine was injected into a micro-model that was saturated with a 10,000 cp oil. Figure 4 shows the fingers formed after 80  $\mu$ l of brine was injected into the system. The fingering is at the pore scale. The finger has a structure like the ones modeled by diffusion limited aggregation (DLA). Side branches form during the growth of the finger, but side branches do not grow much. Water takes the shortest path (path of least resistance) from the inlet to the exit channel. A large portion of the micromodel remains unswept and hence, the recovery is poor. The water injection was stopped after about 2.1 ml of water was injected. Figure 5 shows the final picture of the micromodel at the end of the water flood. A lot of water resides in the side branches of the finger which do not contribute to flow. Only the flowing fraction (a small part of the water saturation) contributes to the flow and hence the water relative permeability tends to be lower than those for light oil displacement for the same porous medium. The oil in pores next to the side branches of the water is also immobile. Therefore the oil relative permeability is lower than those of the light oils at similar saturations [15]. The fractal pattern formed in the process of viscous fingering justifies the observed decrease in both oil and water relative permeability in the case of viscous oils.



Figure 4. Fingers during water flood with  $\mu_r = 10,000$ ; 80  $\mu$ l injected

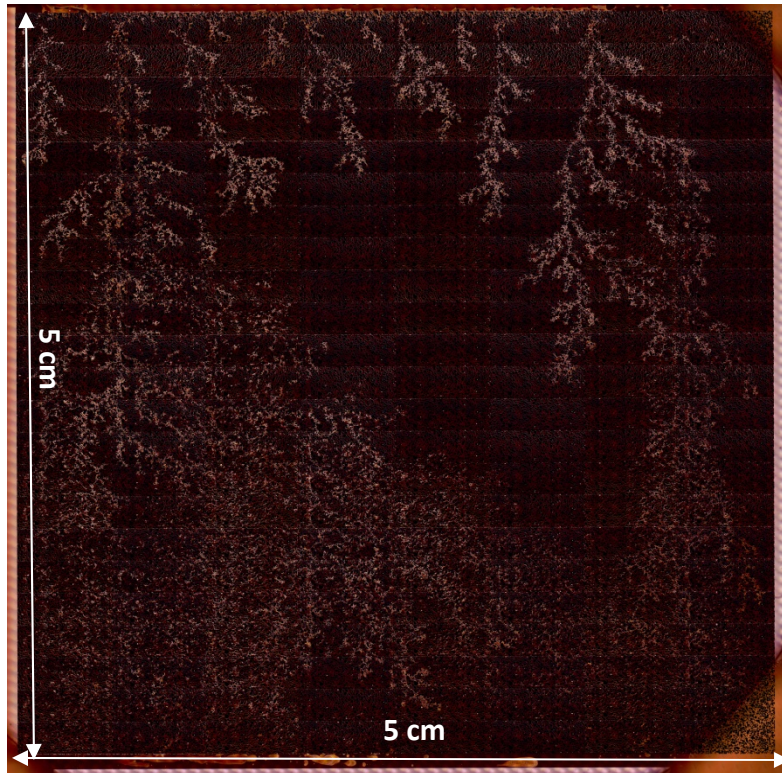


Figure 5. Final state of the micromodel after 2.1 ml of injection,  $\mu_r = 10,000$

10000 cP Oil Displaced by 100 cP Polymer Solution  $\mu_r = 100$

The same 10000 cp oil saturated micromodel was flooded with a 100 cp polymer solution (3000 ppm of HPAM in 2% NaCl). Figure 6 shows the image of the fluid distribution after 80  $\mu$ l of injection. It shows a main finger and a side branch growing simultaneously. The other side branches of the main finger appear smaller than those at a viscosity ratio of 10,000. After the main branch and the side branch breakthrough in the exit channel, other fingers grow and sweep more oil out. Figure 7 shows the picture of the final state of the model after 2.1 ml of polymer solution has been injected. It is clear that many side branches have grown and interconnected water channels have formed all along the model. The viscosity of the polymer increased the stability of the flood but the fractal structures still formed. However, it was noticed that the side branches of the fractal fingers contributed more to the flow in this case. In Expt. 5, a 1000 cp oil was displaced by water at viscosity ratio of 1000. The behavior of the displacement front was in between the cases of 100 and 10,000 viscosity ratios.



Figure 6. Fingers during polymer flood with  $\mu_r = 100$ , 80  $\mu\text{l}$  injected



Figure 7. Final state of the micromodel after 2.1 ml of injection,  $\mu_r = 100$

### **Tertiary Floods**

#### Alkali Surfactant Flooding in the Water and Polymer Flooded Model

An alkali surfactant mixture was prepared as per the composition shown in Table 1. This composition produces an oil-in-water emulsion when mixed in 1:9 ratio of oil to brine, but the emulsion changes to water-in-oil as the oil-water ratio increases [14]. Figure 8(a) shows the state of the micromodel after 2 ml of AS formulation was injected at the end of the waterflood at 10,000 viscosity ratio (Experiment 1). The clear region shows the swept oil region. The water fingers grew and extra oil was recovered. Figure 8(b) shows the state of the micromodel after 2ml of alkaline solution was injected at the end of the polymer flood (Experiment 3). The oil recovery was much higher in the case of polymer flood, because of the highly interconnected network of water channels and higher water oil contact area. This suggests that an alkaline-surfactant flood following a polymer flood would recover more oil than that following a waterflood for a 10,000 cP oil. The pressure drop and production rate may put economic limits to this process.



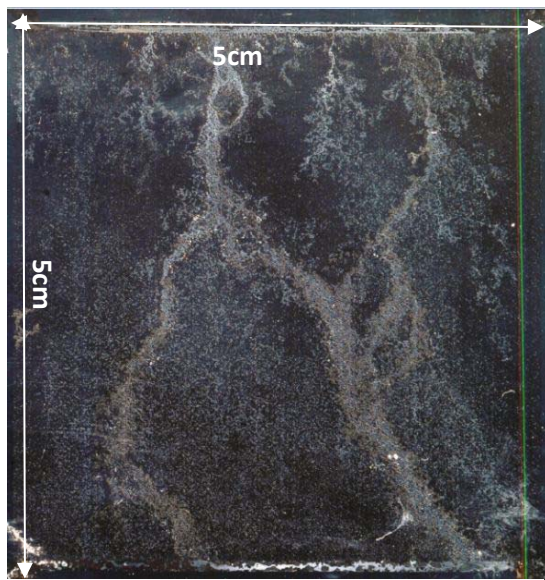


Figure 8(a). Micromodel at the end of AS flood after water flood

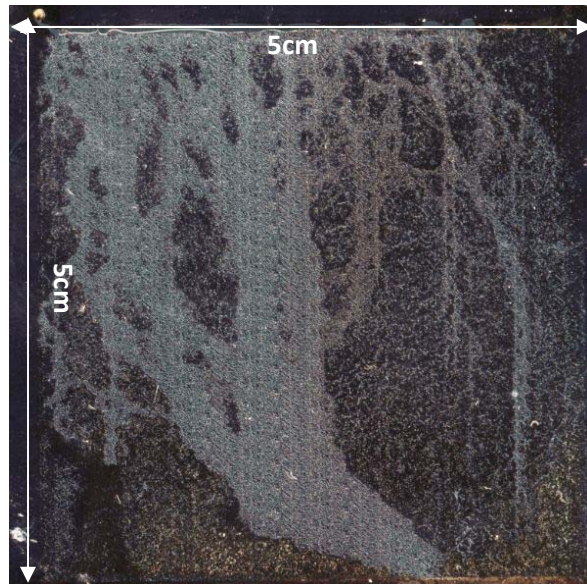


Figure 8(b). Micromodel at the end of AS flood after polymer flood

Figures 8(a) and (b) show broadening of fingers during alkaline-surfactant flood which suggests that oil is pulled out from the sides of the fingers. The alkali surfactant flow was also observed under the microscope to visualize the phenomenon occurring at the pore scale. Figure 9 shows the sequence of pictures that show a blob of trapped oil being pulled out from the sides of flow channels. The structures in white are the sand grains and the trapped oil can be seen as the black patch around the grains. As alkaline-surfactant solution flows through the channel and we see the black oil blob being pulled out into the flow channel. Oil droplets flow through the alkaline-surfactant solutions. These droplets form oil-in-water emulsions.

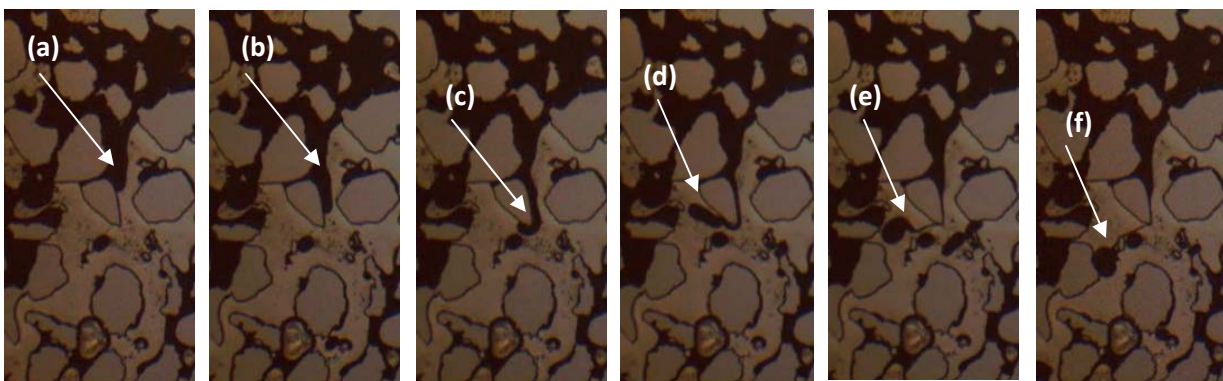


Figure 9. (a-f) Sequence of images showing a blob of trapped oil being pulled out with the alkaline-surfactant solution. (a) Trapped oil left behind after the water flood. (b-c) Trapped oil gets mobilized in contact with the AS slug. (d-e) The mobilized blob of oil is pulled into the flow channel forming a microscopic oil bead. (f) The microscopic oil bead gets dislodged and is washed away by the flow current.

Based on our experimental observations at the pore-scale and the macro-scale, we can propose the following mechanisms for viscous oil displacements. If water (or a polymer solution of viscosity lower than oil) is injected into a viscous oil reservoir, it will finger through the porous medium breaking into the production well. The fingering pattern is fractal, the branching is dependent on the viscosity ratio. The fingers have many side water channels which are immobile surrounded by oil which is also immobile. Wang et al. [18] had reported that the water and oil relative permeabilities of viscous oils were lower than that of those of light oils. This depressed relative permeability originates from these immobile water side branches and the surrounding immobile oil. The depressed relative permeability also keeps water-oil ratio depressed for a long time after the water breakthrough in viscous oils [14]. The oil recovery scaled as the square root of time during waterfloods after finger breakthrough in corefloods [14]. We observe in pore-scale models that the fingers grow by co-current imbibition of water.

As shown in the Figure 10, when the formulated alkali-surfactant slug is injected into the medium it starts interacting with the trapped oil it comes in contact with. The injected surfactant and the in-situ soaps formed by the alkali produce low interfacial tension. The oil drops deform and get pulled into the flow channels causing the fingers to grow in the lateral direction. The oil recovery by this mechanism depends on the amount of oil-water contact area available for the chemical interaction. The polymer flood produces more surface area than the waterflood. Thus the tertiary alkaline-surfactant flood recovers more oil in the case of the polymer flood.

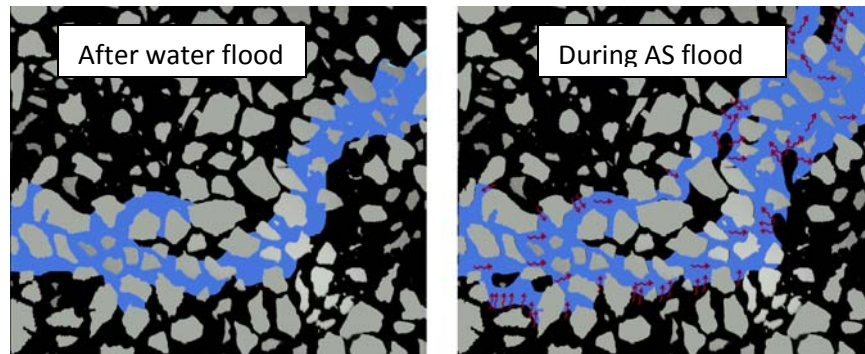


Figure 10. Pore-scale diagram showing the blobs of oil being pulled out in AS flood

## CONCLUSIONS

1. When water displaces viscous oils, fingers form at all scales (pore scale to sample scale). The viscosity ratio controls the finger structure. As the viscosity ratio increases, the number of growing fingers (or branches) before breakthrough decreases. At high viscosity ratios of about  $10^3$  or more, the fingers formed are not completely random but follow a structure of DLA type fractal pattern.
2. The pore-scale fluid distribution of viscous fingers is very different from the invasion-percolation fingers of stable displacements. The branched structure of the pore-scale fingers leads to a decrease in both oil and water relative permeabilities.
3. Injection of alkaline-surfactant solution after waterflood lowers the interfacial tension and forms oil-in-water emulsion at the sides of previously established water fingers.
4. The tertiary oil recovery due to alkaline-surfactant flood increases with the surface area of the water fingers. The tertiary flood after the polymer flood recovers more oil than the tertiary flood following the water flood.

## REFERENCES

1. "Heavy\_Oil\_Fact\_Sheet", *California Department of Oil Gas and Geothermal Resources, United States Federal Government*, June 17, 2006.
2. Coskuner, G., "A New Process Combining Cyclic Steam Stimulation and Steam-Assisted Gravity Drainage: Hybrid SAGD," *Journal of Canadian Petroleum Technology*, 48 (1), 8-13 (2009).
3. Alboudwarej H. et al., "Highlighting Heavy Oil," *Oilfield Review*, 34-53, (Summer 2006)
4. Das, S. K., "Vapex: An Efficient Process for Recovery of Heavy Oil & Bitumen," *SPE Journal*, 3, 232-237 (September, 1998)
5. Kumar, M., Hoang, V. and Satik, C. "High Mobility Ratio Waterflood Performance Prediction: Challenges and New Insights". *SPE Res Eval & Eng*, 11 (1), 186-196 (2005). doi: 10.2118/97671-PA.
6. Paterson, L., "Diffusion-Limited Aggregation and Two-Fluid Displacements in Porous Media." *Physical Review Letters*, 52 (18), 1621 (1984).
7. Chen, J.-D. and D. Wilkinson, "Pore-Scale Viscous Fingering in Porous Media". *Physical Review Letters*, 55 (18), 1892 (1985).
8. Lenormand, R., E. Touboul, and C. Zarcone, "Numerical models and experiments on immiscible displacements in porous media", *Journal of Fluid Mechanics*, 189, 165-187 (1988).

9. Lenormand, R., "Flow Through Porous Media: Limits of Fractal Patterns", *Proceedings of the Royal Society of London. Series A, Mathematical and Physical Sciences*, 423 (1864); 159-168 (1989).
10. Seright, R.S., "Potential for Polymer Flooding with Viscous Oils", *SPEREE*, 13 (4), 730-740 (2010).
11. Hirasaki, G.J., Miller, C.A., and Puerto, M. 2008. "Recent Advances in Surfactant EOR," *SPE 115386 presented at the SPE Annual Technical Conference and Exhibition*, Denver, Colorado, 21-24 September. doi: 10.2118/115386-MS.
12. Flaaten, A.A., Nguyen, Q.P., Zhang, J., Mohammadi, H., and Pope, G.A. 2008. "ASP Chemical Flooding Without the Need for Soft Water". *SPE 116754 presented at the SPE Annual Technical Conference and Exhibition*, Denver, Colorado, 21-24 September. doi: 10.2118/116754-MS.
13. Bryan, J. and Kantzas, A. "Enhanced Oil Recovery by Alkali-Surfactant Flooding". *SPE 110738 presented at the SPE Annual Technical Conference and Exhibition*, Anaheim, CA USA, 11-14 November, 2007. doi: 10.2118/110738-MS.
14. Kumar, R. and K.K. Mohanty, "ASP Flooding of Viscous Oils", *SPE 135265 presented at the SPE Annual Technical Conference and Exhibition*, Florence, Italy, 19-22 September, 2010. doi: 10.2118/135265-MS
15. Ruckenstein, E. *Microemulsions, Macroemulsions, and Bancroft's Rule*, *Langmuir*, 12 (26), 6351-6353 (1996).
16. Sun, W., Z. Qu, and G.-Q. Tang, "Characterization of Water Injection in Low Permeable Rock Using Sandstone Micro-Model", *SPE 86964, SPE International Thermal Operations and Heavy Oil Symposium and Western Regional Meeting*, Bakersfield, CA, 16-18 March, 2004.
17. Alshehri, A., E. Sagatov, and A.R. Kovscek, "Pore-Level Mechanics of Forced and Spontaneous Imbibition of Aqueous Surfactant Solutions in Fractured Porous Media", *SPE 124946, SPE ATCE*, New Orleans, LA, 4-7 October, 2009.
18. Wang, J., M. Dong, and K. Asghari, "Effect of Oil Viscosity on Heavy Oil-Water Relative Permeability Curves", *SPE 99763, presented in SPE/DOE Symposium on Improved Oil Recovery*. Tulsa, Oklahoma, 22-26 April, 2006. doi: 10.2118/99763-MS